USING DUAL FORMULATIONS FOR CORRECTION OF THIN SHELL MAGNETIC MODELS BY A FINITE ELEMENt SUBPROBLEM METHOD

Dang Quoc Vuong[1], Bui Duc Hung[1], Khuong Van Hai[2]

[1]*Hanoi University of Science and Technology; vuong.dangquoc@hust.edu.vn*

[2]*Water Resources University*

Abstract - Dual formulations for finite element magnetostatic and magnetodynamic subproblems are developed to correct the inaccuracies near edges and corners of thin shell magnetic models. Such models replace volume thin regions by surfaces but neglect border effects in the vicinity of their edges and corners, which can cause inaccuracy in solving thin sheel problems. The developed surface-to-volume correction problem is defined as a step of the multiple subproblems applied to a complete problem (inductors and conductor regions), considering successive additions of inductors and magnetic or conducting regions, some of which are thin regions. Each subproblem is independently solved on its own domain and mesh, which facilitates meshing and increases computational efficiency.

Key words - Eddy current, finite element method (FEM), magnetodynamics, subproblem method (SPM), thin shell (TS)

1. Introduction

As proposed in [1], [2], thin shell (TS) finite element (FE) models are used to avoid meshing thin regions, which are replaced by surfaces with interface conditions (ICs). Nevertheless, these ICs lead to inaccuracies on the computation of local electromagnetic quantities (current density, magnetic flux density and magnetic field) in the vicinity of geometrical discontinuities (edges and corners). Such inaccuracies increase with the thickness, and are exhacerbated for quadratic quanti-ties like forces and Joule losses, which are often the primary quantities of interest. To cope with these disadvantages, a subproblem method (SPM) based on magnetic flux density formulations, proposing a surface-to-volume local correction, has been proposed in [3]. The SPM for TS correction is explicitly developed for dual finite element (FE) ***b***- and ***h***- formulations, with generalized mesh projections of solutions between the subproblems (SPs). Also, the SPM naturally allows parameterized analyses of the thin region characteristics: permeability, conductivity and thickness. In the proposed SP strategy, a reduced problem (SP *u*) with only inductors is first solved on a simplified mesh without thin and volume regions. Its solution gives surface sources (SSs) as ICs for added TS regions (SP *p*), and volume sources (VSs) for possible added volume regions (SP k). The TS solution is then corrected by a volume correction via SSs and VSs that suppress the TS representation and add the volume model. The method allows coupling SPs in two procedures: one-way coupling and two-way coupling. The one-way coupling is a SP sequence, where no iteration between the SPs is necessary. On the other hand, with two-way coupling, each SP solution is influenced by all the others, which thus must be included in an iterative process.

2. Thin Shell Correction in a SPM

2.1. Canonical magnetodynamic or static problem

A canonical magnetodynamic problem *i*, to be solved at step *i* of the SPM ($i \equiv u$, *p or k*), is defined in a domain Ω_i, with boundary $\partial\Omega_i = \Gamma_i = \Gamma_{h,i} \cup \Gamma_{b,i}$. The eddy current conducting part of Ω_p is denoted $\Omega_{c,p}$ and the non-conducting one $\Omega^C{}_{c,i}$, with $\Omega_i = \Omega_{c,i} \cup \Omega^C{}_{c,i}$. Stranded inductors belong to $\Omega^C{}_{c,i}$, whereas massive inductors belong to $\Omega_{c,i}$. The equations, material relations and boundary conditions (BCs) of SP *i* are

$$\operatorname{curl} \boldsymbol{h}_i = \boldsymbol{j}_i\,,\ \ \operatorname{div} \boldsymbol{b}_i = 0,\ \ \operatorname{curl} \boldsymbol{e}_i = -\partial_t \boldsymbol{b}_i \qquad (1a-b-c)$$

$$\boldsymbol{h}_i = \mu_i^{-1} \boldsymbol{b}_i + \boldsymbol{h}_{s,i}\,,\ \ \boldsymbol{j}_i = \sigma_i \boldsymbol{e}_i + \boldsymbol{j}_{s,i} \qquad (2a-b)$$

$$\boldsymbol{n} \times \boldsymbol{h}_i\big|_{\Gamma_{h,i}} = \boldsymbol{j}_{f,i}\,,\ \ \boldsymbol{n} \cdot \boldsymbol{b}_i\big|_{\Gamma_{b,i}} = \boldsymbol{f}_{f,i} \qquad (3a-b)$$

$$\boldsymbol{n} \times \boldsymbol{e}_i\big|_{\Gamma_{e,i} \subset \Gamma_{b,i}} = \boldsymbol{k}_{f,i} \qquad (3c)$$

where $\boldsymbol{h}_i$ is the magnetic field, $\boldsymbol{b}_i$ is the magnetic flux density, $\boldsymbol{e}_i$ is the electric field, $\boldsymbol{j}_i$ is the electric current density, μ_i is the magnetic permeability, σ_i is the electric conductivity and $\boldsymbol{n}$ is the unit normal exterior to Ω_i. The field $\boldsymbol{h}_{s,i}$ and $\boldsymbol{j}_{s,i}$ and in (2a) and (2b) are VSs that can be used for expressing changes of a material property in a volume region [3]. The fields $\boldsymbol{j}_{f,i}$ and $\boldsymbol{k}_{f,i}$ in (3a) and (3b) are SSs and generally equal zero for classical homogeneous BCs. ICs can define their discontinuities through any interface γ_i (γ_i^+ and γ_i^-) in Ω_i, with the notation $[\,\cdot\,]_{\gamma_i} = \cdot|_{\gamma_i^+} - \cdot|_{\gamma_i^-}$. If nonzero, they define possible SSs that account for particular phenomena occurring in the idealized thin region between γ_i^+ and γ_i^- [3]. This is the case when some field traces in SP p are forced to be discontinuous (e.g. in TS model), whereas their continuity must be recovered via a SP *k*; with the SSs fixed as the opposite of the trace discontinuity solution of SP *p*.

2.2. Subproblem:"Adding a thin shell"

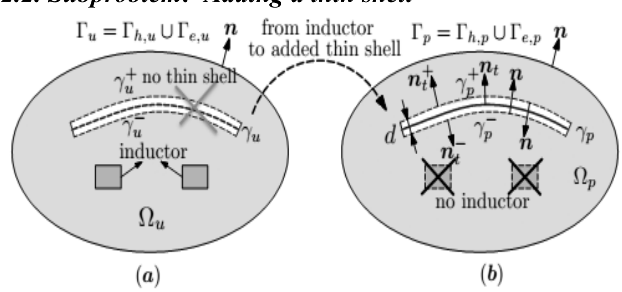

Figure 1*: Interface condition between SP u and SP p*

The solution of an SP *u* is first known for a particular configuration, e.g. for an inductor alone (Figure 1, a), or more generally resulting from the superposition of several SP solutions. The next SP *p* consists in adding a TS to this configuration (Figure 1, b). From SP *u* to SP *p*, the solution *u* gives SSs for the added TS γ_p, through TS ICs [2]. The ***b***-formulation uses a magnetic vector potential $\boldsymbol{a}_i$ (such that curl $\boldsymbol{a}_i = \boldsymbol{b}_i$), split as $\boldsymbol{a} = \boldsymbol{a}_{c,i} + \boldsymbol{a}_{d,i}$ [2]. The ***h***-formulation uses a similar splitting for the magnetic field, $\boldsymbol{h} = \boldsymbol{h}_{c,i} + \boldsymbol{h}_{d,i}$. The fields $\boldsymbol{a}_{c,i}$, $\boldsymbol{h}_{c,i}$ and $\boldsymbol{a}_{d,i}$, $\boldsymbol{h}_{d,i}$ are continuous and discontinuous respectively through the TS. The traces discontinuities in SP p $[\boldsymbol{n}\times\boldsymbol{h}_p]_{\gamma_p}$ and $[\boldsymbol{n}\times\boldsymbol{e}_p]_{\gamma_p}$ (with $\boldsymbol{n}_t = -\boldsymbol{n}$) in both formulations can be expressed as paper [2]

$$[\boldsymbol{n}\times(\boldsymbol{h}_u\times\boldsymbol{h}_p)]_\gamma = [\boldsymbol{n}\times\boldsymbol{h}_p]_{\gamma_p} = \mu_p\beta_p\partial_t(2\boldsymbol{a}_{c,p}+\boldsymbol{a}_{d,p}) \quad (4)$$

$$[\boldsymbol{n}\times(\boldsymbol{e}_u\times\boldsymbol{e}_p)]_\gamma = [\boldsymbol{n}\times\boldsymbol{e}_p]_{\gamma_p} = \sigma_p\beta_p\partial_t(2\boldsymbol{h}_{c,p}+\boldsymbol{h}_{d,p}) \quad (5)$$

$$\beta_p = \theta_p^{-1}\tanh(\theta_p.d_p/2),\ \theta_p = (1+j)/\delta_p \quad (6)$$

because there are no discontinuities in SP u (before adding γ_p), where d_p is the local TS thickness, $\delta_p = \sqrt{2/(\omega\sigma_p\mu_p)}$ is the skin depth in the TS, $\omega = 2\pi f$, f is the frequency and j is the imaginary unit. Also, the traces of $\boldsymbol{e}_p$ and $\boldsymbol{h}_p$ on the positive side γ_p^+ are expressed as [2]

$$\boldsymbol{n}\times\boldsymbol{h}_p\big|_{\gamma^+_p} = \frac{1}{2}[\sigma_p\beta_p\partial_t(2\boldsymbol{a}_{c,p}+\boldsymbol{a}_{d,p}) + \frac{1}{\sigma_p\beta_p}\boldsymbol{a}_{d,p}] - \boldsymbol{n}\times\boldsymbol{h}_u\big|_{\gamma^+_p} \quad (7)$$

$$\boldsymbol{n}\times\boldsymbol{e}_p\big|_{\gamma^+_p} = \frac{1}{2}[\mu_p\beta_p\partial_t(2\boldsymbol{h}_{c,p}+\boldsymbol{h}_{d,p}) + \frac{1}{\sigma_p\beta_p}\boldsymbol{a}_{d,p}] - \boldsymbol{n}\times\boldsymbol{e}_u\big|_{\gamma^+_p} \quad (8)$$

2.3. Subproblem: "Correcting a thin shell"

A TS solution obtained in an SP p can be further improved by a volume correction SP k via SSs and VSs that overcome the TS assumptions. SP k has to suppress the TS representation via SSs opposed to TS discontinuities, in parallel with VSs in the added actual volume that account for changes of material properties in the added volume region from μ_p and σ_p in SP p to from μ_k and σ_k in SP k (with $\mu_p = \mu_0$, $\mu_k = \mu_{volume}$, $\sigma_k = 0$ and $\sigma_k = \sigma_{volume}$). This defines a surface-to-volume correction. Such a correction generally leads to local modifications of the solution, which thus allows reducing the calculation domain and its mesh in the surroundings of the thin regions. The VSs for SP k are paper [3]

$$\boldsymbol{b}_{s,k} = (\mu_k - \mu_p)(\boldsymbol{h}_u + \boldsymbol{h}_p),\ \boldsymbol{j}_{s,k} = (\sigma_p - \sigma_p)(\boldsymbol{e}_{c,p} + \boldsymbol{e}_{d,p}) \quad (9a\text{-}b)$$

$$\boldsymbol{h}_{s,k} = (\mu^{-1}{}_k - \mu^{-1}{}_p)(\boldsymbol{b}_u + \boldsymbol{b}_p),\ \boldsymbol{e}_{s,k} = -(\boldsymbol{e}_{c,p} + \boldsymbol{e}_{d,\ }) \quad (10a\text{-}b)$$

3. Finite Element Weak Formulations

3.1. Magnetic Vector Potential Formulation

The weak $\boldsymbol{b}_i$ -formulation (in terms of $\boldsymbol{a}_i$) of SP i ($i \equiv u$, p or k) is obtained from the weak form of the Ampère equation (1a), i.e. [3], [4]

$$(\mu_i^{-1}\,\mathrm{curl}\,\boldsymbol{a}_i, \mathrm{curl}\,\boldsymbol{a}_i')_{\Omega_i} + (\boldsymbol{h}_{s,i}, \mathrm{curl}\,\boldsymbol{a}_i')_{\Omega_i} + (\boldsymbol{j}_{s,i}, \boldsymbol{a}_i')_{\Omega_i} + (\sigma_i\,\partial_t\,\boldsymbol{a}_i, \boldsymbol{a}_i')_{\Omega_i} + \langle\boldsymbol{n}\times\boldsymbol{h}_i, \boldsymbol{a}_i'\rangle_{\Gamma_{h,i}-\Gamma_{t,i}} + \langle[\boldsymbol{n}\times\boldsymbol{h}_i]_{\Gamma_{t,i}}, \boldsymbol{a}_i'\rangle_{\Gamma_{t,i}} = (\boldsymbol{j}_{s,i}, \boldsymbol{a}_i')_{\Omega_i}, \forall\boldsymbol{a}_i' \in F_i^1(\Omega_i) \quad (11)$$

where $F_i^1(\Omega_i)$ is a curl-conform function space defined in Ω_i, gauged in $\Omega_{c,i}^C$, and containing the basis functions for $\boldsymbol{a}$ as well as for the test function $\boldsymbol{a}_i'$ (at the discrete level, this space is defined by edge FEs; the gauge is based on the tree-co-tree technique); $(\cdot,\cdot)_\Omega$ and $\langle\cdot,\cdot\rangle_\Gamma$ respectively denote a volume integral in Ω and a surface integral on Γ of the product of their vector field arguments. The surface integral term on $\Gamma_{h,i}$ accounts for natural BCs of type (3a), usually zero. At the discrete level, the required meshes for each SP i differ.

3.1.1. Inductor alone - SP u

The weak form of an SP u with the inductor alone is first solved via the first and last volume integrals in (11) ($i \equiv u$) where $\boldsymbol{j}_i$ is the fixed current density in on Ω_s.

3.1.2. Thin shell FE model- SP p

The TS model is defined via the term $\langle[\boldsymbol{n}\times\boldsymbol{h}_p]_{\gamma_p}, \boldsymbol{a}_{d,p}'\rangle_{\gamma_p}$ in (11) ($i \equiv p$). The test function $\boldsymbol{a}_i'$ is split into continuous and discontinuous parts $\boldsymbol{a}'_{c,p}$ and $\boldsymbol{a}'_{d,p}$ (with $\boldsymbol{a}'_{d,p}$ zero on γ^-_p) [2]. One thus has

$$\langle[\boldsymbol{n}\times\boldsymbol{h}_p]_{\gamma_p}, \boldsymbol{a}_p'\rangle_{\gamma_p} = \langle[\boldsymbol{n}\times\boldsymbol{h}_p]_{\gamma_p}, \boldsymbol{a}_{c,p}'\rangle_{\gamma_p} + \langle\boldsymbol{n}\times\boldsymbol{h}_p|_{\gamma^+_p}, \boldsymbol{a}_{d,p}'\rangle_{\gamma^+_p} \quad (12)$$

The terms of the RHS of (12) are developed using (4) and (7) respectively, i.e.

$$\langle[\boldsymbol{n}\times\boldsymbol{h}_p]_{\gamma_p}, \boldsymbol{a}_{c,p}'\rangle_{\gamma_p} = \langle[\boldsymbol{n}\times\boldsymbol{h}]_{\gamma_p}, \boldsymbol{a}_{c,p}'\rangle_{\gamma_p} = \langle\sigma_p\beta_p\partial_t(2\boldsymbol{a}_{c,p}+\boldsymbol{a}_{d,p}), \boldsymbol{a}_{c,p}'\rangle_{\gamma_p} \quad (13)$$

$$\langle[\boldsymbol{n}\times\boldsymbol{h}_p]_{\gamma^+_p}, \boldsymbol{a}_{d,p}'\rangle_{\gamma_p} = -\langle\boldsymbol{n}\times\boldsymbol{h}_u|_{\gamma^+_p}, \boldsymbol{a}_{d,p}'\rangle_{\gamma^+_p} + \frac{1}{2}\langle\sigma_p\beta_p\partial_t(2\boldsymbol{a}_{c,p}+\boldsymbol{a}_{d,p}) + \frac{1}{\sigma_p\beta_p}, \boldsymbol{a}_{d,p}'\rangle_{\gamma_p} \quad (14)$$

The last surface integral term in (14) is related to a SS that can be naturally expressed via the weak formulation of SP u (11), i.e.

$$-\langle\boldsymbol{n}\times\boldsymbol{h}_u|_{\gamma^+_p}, \boldsymbol{a}_{d,p}'\rangle_{\gamma^+_p} = (\mu_u^{-1}\,\mathrm{curl}\,\boldsymbol{a}_u, \mathrm{curl}\,\boldsymbol{a}_{d,p}')_{\Omega^+_p}$$

At the discrete level, the volume integral in (15) is thus limited to a single layer of FEs on the side Ω^+_p touching γ_p^+, because it involves only the associated trace $\boldsymbol{n}\times\boldsymbol{a}_{d,p}'|_{\gamma^+_p}$. Also, the source $\boldsymbol{a}_u$, initially in the mesh of SP u, has to be projected on the mesh of SP p, using a projection method [5].

3.1.3. Volume correction replacing the TS representation - SP k

The TS SP p solution is then corrected by SP k via the volume integrals $(\boldsymbol{h}_{s,p}, \mathrm{curl}\,\boldsymbol{a}')_{\Omega_p}$ and $(\boldsymbol{j}_{s,p}, \boldsymbol{a}')_{\Omega_p}$ in (11). The VSs $\boldsymbol{j}_{s,k}$ and $\boldsymbol{h}_{s,k}$ are given in (9) and (10), respectively.

Simultaneously to the VSs in (11), SSs have to suppress the TS discontinuities, with ICs to be defined as $[\boldsymbol{n}\times\boldsymbol{h}_k]_{\gamma_k} = -[\boldsymbol{n}\times\boldsymbol{h}_p]_{\gamma_k}$ and $[\boldsymbol{n}\times a]_{\gamma_k} = -[\boldsymbol{n}\times a_p]_{\gamma_k}$. The trace discontinuity $[\boldsymbol{n}\times\boldsymbol{h}_k]_{\gamma_k}$ occurs in (11) via

$$\langle[\boldsymbol{n}\times\boldsymbol{h}_k]_{\gamma_k}, \boldsymbol{a}_k'\rangle_{\gamma_p} = -\langle[\boldsymbol{n}\times\boldsymbol{h}_p]_{\gamma_k}, \boldsymbol{a}_k'\rangle_{\gamma_k} \quad (16)$$

and can be weakly evaluated from a volume integral from SP p similarly to (15). However, directly using the explicit form (4) for $[\boldsymbol{n}\times\boldsymbol{h}_p]_{\gamma_k}$ gives the same contribution, which is thus preferred.

3.2. Magnetic Field Formulation

3.2.1. *h*-Formulation with source and reaction magnetic fields

The $\boldsymbol{h}_i - \phi_i$ formulation of SP i ($i \equiv u$; p or k) is obtained from the weak form of Faraday's law (1 c) [6]. The field $\boldsymbol{h}_i$ is split into two parts, $\boldsymbol{h}_i = \boldsymbol{h}_{s,i} + \boldsymbol{h}_{r,i}$ where $\boldsymbol{h}_{s,i}$ is a source field defined by curl $\boldsymbol{h}_{s,i} = \boldsymbol{j}_{s,i}$ and $\boldsymbol{h}_{r,i}$ is unknown. One has

$$\partial_t(\mu_i(\boldsymbol{h}_{r,i}+\boldsymbol{h}_{s,i}),\boldsymbol{h}_i')_{\Omega_i}+(\sigma_i^{-1}\,\mathrm{curl}\,\boldsymbol{h}_i,\mathrm{curl}\,\boldsymbol{h}_i')_{\Omega_i}+$$
$$\partial_t(b_{s,i},\boldsymbol{h}_i')_{\Omega_i}+(e_{s,i},\mathrm{curl}\,\boldsymbol{h}_i')_{\Omega_i}+<\boldsymbol{n}\times e_i,\boldsymbol{h}_i'>_{\Gamma_{e,i}}$$
$$+<[\boldsymbol{n}\times e_i]_{\gamma_i},\boldsymbol{h}_i'>_{\gamma_i}=0,\forall\,\boldsymbol{h}_i'\in F_i^1(\Omega_i)$$

where $F_i^1(\Omega_i)$ is a curl-conform function space defined in Ω_i and contains the basis functions for $\boldsymbol{h}_i$ as well as for the test function $\boldsymbol{h}_i'$. The surface integral term on $\Gamma_{e,i}$ accounts for natural BCs of type (3 b), is usually zero.

3.2.2. Inductor model SP u

The model SP u with only the inductor is first solved with (17) ($i \equiv p$). The source field $\boldsymbol{h}_{s,u}$ is defined via a projection method of a known distribution $\boldsymbol{j}_{s,u}$ [5], i.e

$$(\mathrm{curl}\,\boldsymbol{h}_{s,u},\mathrm{curl}\,\boldsymbol{h}_{s,u}')_{\Omega_u}=(j_{s,u},\mathrm{curl}\,\boldsymbol{h}_{s,u}')_{\Omega_u},$$
$$\forall\,\boldsymbol{h}_{s,u}'\in F_u^1(\Omega_u) \quad (18)$$

3.2.3. Thin shell FE model - SP p

The TS model is defined via the term $<[\boldsymbol{n}\times e_p]_{\gamma_p},\boldsymbol{h}_{d,p}'>_{\gamma_p}$ in (11) ($i \equiv p$). The test function $\boldsymbol{h}_i'$ is split into continuous and discontinuous parts $\boldsymbol{h}'_{c,p}$ and $\boldsymbol{h}'_{d,p}$ (with $\boldsymbol{h}'_{d,p}$ zero on γ^-_p) [2]. One thus has

$$<[\boldsymbol{n}\times e_p]_{\gamma_p},\boldsymbol{h}_p'>_{\gamma_p}=<[\boldsymbol{n}\times e_p]_{\gamma_p},\boldsymbol{h}_{c,p}'>_{\gamma_p}+$$
$$<\boldsymbol{n}\times e_p|_{\gamma^+_p},\boldsymbol{h}_{d,p}'>_{\gamma^+_p}. \quad (19)$$

The terms of the right-hand side of (19) are developed using (5) and (8) respectively, i.e.

$$<[\boldsymbol{n}\times e_p]_{\gamma_p},\boldsymbol{h}_{c,p}'>_{\gamma_p}=<[\boldsymbol{n}\times e]_{\gamma_p},\boldsymbol{h}_{c,p}'>_{\gamma_p}$$
$$=<\mu_p\beta_p\partial_t(2\boldsymbol{h}_{c,p}+\boldsymbol{h}_{d,p}),\boldsymbol{h}_{c,p}'>_{\gamma_p}, \quad (20)$$
$$<[\boldsymbol{n}\times e_p]_{\gamma^+_p},\boldsymbol{h}_{d,p}'>_{\gamma_p}=-<\boldsymbol{n}\times e_u|_{\gamma^+_p},\boldsymbol{h}_{d,p}'>_{\gamma^+_p}+$$
$$\frac{1}{2}<\mu_p\beta_p\partial_t(2\boldsymbol{h}_{c,p}+\boldsymbol{h}_{d,p})+\frac{1}{\mu_p\beta_p},\boldsymbol{h}_{d,p}'>_{\gamma_p} \quad (21)$$

The last surface integral term in (21) is related to a SS that can be naturally expressed via the weak formulation of SP *u* (17), i.e.

$$-<\boldsymbol{n}\times e_u|_{\gamma^+_p},\boldsymbol{h}_{d,p}'>_{\gamma^+_p}=(\mu_u\partial_t(\boldsymbol{h}_{s,u}+\boldsymbol{h}_{s,u}),\boldsymbol{h}_{d,p}')_{\Omega^+_p} \quad (22)$$

The sources $\boldsymbol{h}_{s,i}$ and $\boldsymbol{h}_{r,i}$, initially in the mesh of SP *u*, have to be projected on the mesh of SP *p* using a using a projection method [5].

3.2.4. Volume correction replacing the TS representation SP k

Once obtained, the TS solution in SP *p* is corrected by SP *k* via the volume integrals $\partial_t(b_{s,p},\boldsymbol{h}')_{\Omega_p}$ and $(e_{s,p},\mathrm{curl}\,\boldsymbol{h}_k')_{\Omega_k}$. The VSs $\boldsymbol{b}_{s,k}$ and $\boldsymbol{e}_{s,k}$ are also given in (9) and (10), respectively. The VS $\boldsymbol{e}_{s,k}$ in (10) is to be obtained from the still unknown electric fields $\boldsymbol{e}_u$ and $\boldsymbol{e}_p$ and their determination needs to solve an electric problem [6].

In parallel with the VSs in (17), ICs compensate the TS discontinuities to suppress the TS representation via SSs opposed to previous TS ICs, i.e., $\boldsymbol{h}_{d,k} = -\boldsymbol{h}_{d,k}$ to be strongly defined, and $[\boldsymbol{n}\times e_p]_{\gamma_k}=-[\boldsymbol{n}\times e_p]_{\gamma_k}$. The trace discontinuity $[\boldsymbol{n}\times e_p]_{\gamma_k}$ occurs in (17) via

$$<[\boldsymbol{n}\times e_k]_{\gamma_k},\boldsymbol{h}_k'>_{\gamma_p}=-<[\boldsymbol{n}\times e_p]_{\gamma_k},\boldsymbol{h}_k'>_{\gamma_k} \quad (23)$$

and can be weakly evaluated from a volume integral from SP p similarly to (22).

4. Application Examples

A 3-D test problem is based on TEAM problem 21 (model B, coil and plate, Figure 2).

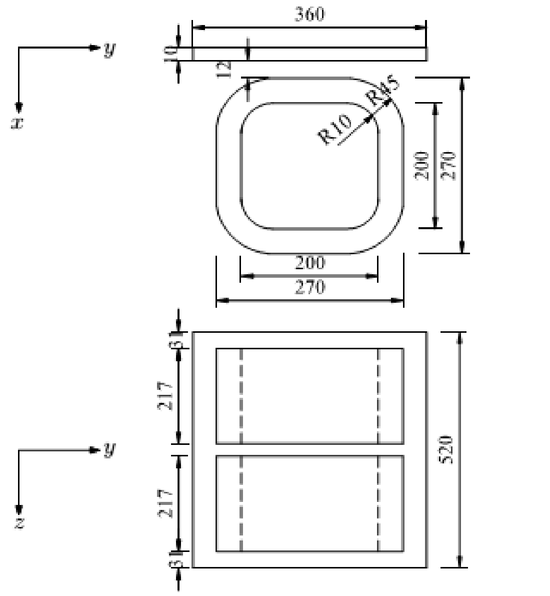

Figure 2. *Geometry of TEAM (Testing Electro-magnetic Analysis Methods) problem 21 – Model B [8]*

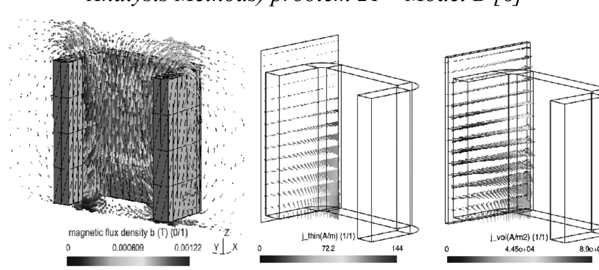

Figure 3. *TEAM problem 21 (1/4th of the geometry): magnetic flux density* $\boldsymbol{b}_u$ *(in a cut plane) generated by a stranded inductor (left), eddy current density* $\boldsymbol{j}_p$ *on TS model (middle) and its volume correction* $\boldsymbol{j}_k$ *(right) (thickness d = 10 mm)*

An SP scheme considering three SPs is developed. A first FE SP *u* with the stranded inductors alone is solved on a simplified mesh without any thin region (Figure 3, *left*). Then an SP *p* is solved with the added thin region via a TS FE model (Figure 3, *middle*). At last, a SP k replaces the TS FEs with the actual volume FEs (Figure 3, *right*). The inaccuracies on the Joule power loss densities of TS SP *p* are pointed out by the importance of the correction SP *k* (Figure 4). Significant error on TS SP *p* along the z-direction reaches 73% near the plate ends (Figure 4, *top*) or 85% along the *y*-direction (Figure 4, *bottom*) with $\delta = 2.1$ mm and thickness d = 7.5mm for both cases. For d = 1.5mm, it is reduced to below 10%. In particular, accurate local corrections with volume correction SP *k* are checked to be close to the reference solution computed from the FEM.

Table I shows the Joule losses in the plate with an approximate BC for SP k. The exterior boundary of SP k is first chosen at a distance $D_{bound} = 200d$ from the thin region, with thickness $d = 10$ mm. The inaccuracies on Joule losses for TS SP *p* reach 58.9%, or 1.2% for volume correction SP *k*, with $f = 50$ Hz, $\mu = 100$ and $\sigma = 6.484$ MS/m in both cases. The proposed SP strategy allows locally focusing on the mesh of volume correction SP *k* and its neighborhood. It is shown that even if D_{bound} is reduced to $2d$, the error on SP k is 1.53%, which is still very accurate. For d = 1mm, the errors on Joule losses for SP p are reduced to 1.17%, or 0.05% for SP *k*. or 0.05% for SP *k*.

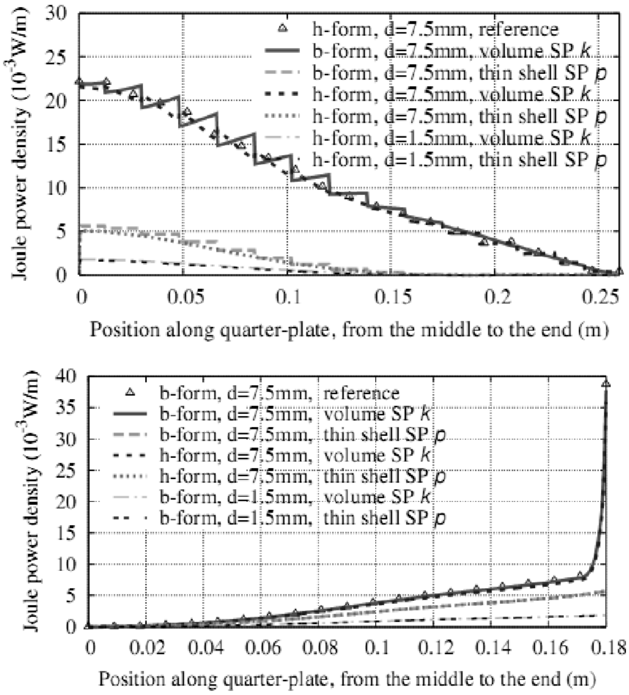

Figure 4. *Power loss density with TS and volume solutions along the z-direction (top) and along the y-direction (bottom), with effects of d (f = 50 Hz, μ_r = 200, σ = 6.484 MS/m)*

The second test problem is a convergence test of two-way coupling (f = 50 Hz, $\mu_r = 1$, $\sigma = 59$ MS/m) (Figure 5). The test at hand is considered in five SPs. It is first solved via an SP *u* with the stranded inductor alone, then adding a TS FE SP p_1 that does not include the stranded inductor via SP *u* with a stranded inductor alone, then adding a TS FE SP p_1 that does not include the stranded inductor anymore. An SP k_1 then replaces the TS SP p_1 with an actual volume covering the plate 1. Next, another TS SP p_2 is added.

Table 1*. Joule losses in the plate with approximate BCs (f = 50 Hz, μ = 100, σ = 6.484 MS/m), with with b- formulation*

D_{bound}	d = 10 mm			Errors %	
	TS P_{thin} (W)	Vol P_{vol} (W)	Ref P_{ref} (W)	Between P_{thin} and P_{ref}	Between P_{vol} and P_{ref}
200*d*	0.0196	0.0477	0.0483	58.9	1.2
20*d*	0.0196	0.0476	0.0483	58.9	1.35
2*d*	0.0196	0.0475	0.0483	58.9	1.53
	d = 1 mm				
200*d*	0.0113	0.0115	0.0115	1.74	0.0001
2*d*	0.0113	0.0115	0.0115	1.77	0.05

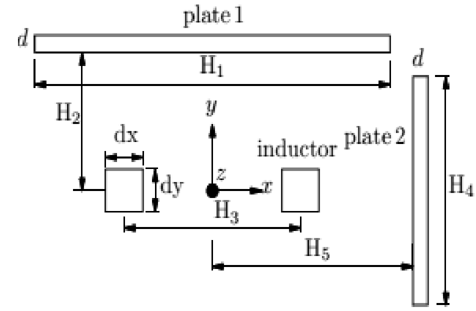

Figure 5. *2-D geometry of an inductor and two plates (d = 5mm, H1 = 120mm, H2 = H3 = 45mm, H4 = 80mm, H5 = 67.5mm, dx = dy = 12mm)*

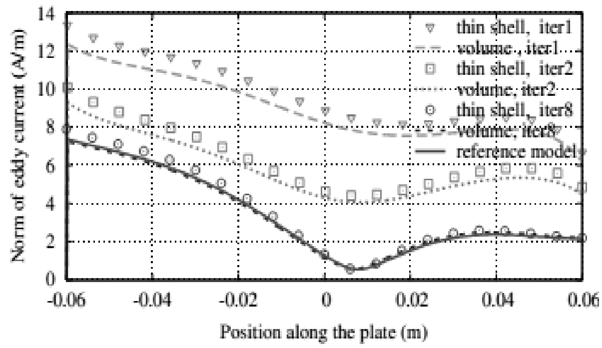

Figure 6. *Norm of the eddy current density **j** (A/m) along the plate 1 at different iterations*

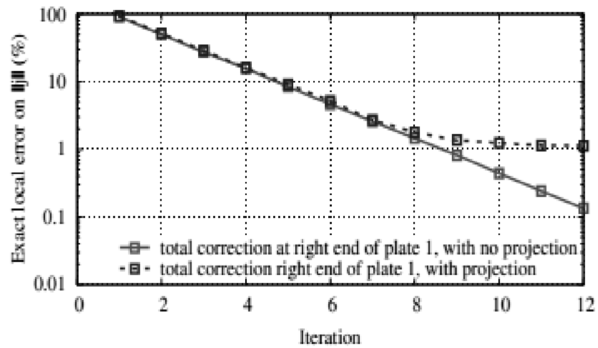

Figure 7. *Exact local errors (top) on the norm of eddy current **j** between the total solution and the reference solution at right end of plate 1, with the number of iterations.*

An SP k_2 eventually replaces the TS SP p_2 with another actual volume covering the plate 2. In the correction process of SP p_1, the fields generated by SP p_2 and SP k_2 are reaction fields that influence the source solutions calculated from previous SP p_1. This means that some iterations between the SPs are required to determine an accurate solution considered as a series of corrections. The problem is first tested on the same mesh to avoid an additional error due to mesh-to-mesh projections. It is then solved with different meshes taking the projection errors into account. Figure 6 represents the convergence of the TS solution SP p_1 and volume solution SP k_1 along the plate 1, for different iterations. The accurate local volume solution is checked to be close to the reference solution during 8 iterations. Relative local errors on the norm of eddy current ***j*** between the total solution and the reference solution at the right end of plate 1 are shown in Figure 7. The error is less than 1% (0.78%) with no projection, and increases slightly up to 1.17% with projection error, during 9 iterations for both cases.

5. Conclusions

The SPM allows correcting the inaccuracies proper to the TS model. Accurate eddy current and power loss densities are obtained, especially along the edges and corners of the thin regions, also for significant thicknesses. The refined mesh for volume correction can be reduced to a close neighborhood of the thin region.

ACKNOWLEDGMENT

This work was supported by the fund of Hanoi University of Science and Technology (HUST).

REFERENCES

[1] L. Krähenbühl and D. Muller, "Thin layers in electrical engineering. Examples of shell models in analyzing eddy-currents by boundary and finite element methods", *IEEE Trans. Magn.*, Vol. 29, No. 2, pp. 1450-1455, 1993.

[2] C. Geuzaine, P. Dular, and W. Legros, "Dual formulations for the modeling of thin electromagnetic shells using edge elements", IEEE Trans. Magn., vol. 36, no. 4, pp. 799–802, 2000.

[3] C. Geuzaine, P. Dular, and W. Legros, "Dual formulations for the modeling of thin electromagnetic shells using edge elements", IEEE Trans. Magn., vol. 36, no. 4, pp. 799–802, 2000.

[4] P. Dular, Vuong Q. Dang, R. V. Sabariego, L. Krähenbühl and C. Geuzaine, "Correction of thin shell finite element magnetic models via a subproblem method", IEEE Trans. Magn., Vol. 47, no. 5, pp. 158 –1161, 2011.

[5] P. Dular, R. V. Sabariego, M. V. Ferreira da Luz, P. Kuo-Peng and L. Krähenbühl, "Perturbation Finite Element Method for Magnetic Model Refinement of Air Gaps and Leakage Fluxes", IEEE Trans. Magn., vol.45, no. 3, pp. 1400-1403, 2009.

[6] C. Geuzaine, B. Meys, F. Henrotte, P. Dular and W. Legros, "A Galerkin projection method for mixed finite elements", IEEE Trans. Magn., Vol. 35, No. 3, pp. 1438-1441, 1999.

[7] P. Dular and R. V. Sabariego, "A perturbation method for computing field distortions due to conductive regions with h-conform magnetodynamic finite element formulations", IEEE Trans. Magn., vol. 43, no. 4, pp. 1293-1296, 2007.

[8] Zhiguang CHENG and Norio TAKAHASHI and Behzad FORGHANI "TEAM Problem 21 Family". Approved by the International Compumag Society Board at Compumag-2009, Florianópolis, Brazil.

(The Board of Editors received the paper on 25/02/2016, its review was completed on 26/04/2016)